Lipid–Protein Multiple Binding Equilibria in Membranes†

Jaakko R. Brotherus,‡ O. Hayes Griffith,* Martti O. Brotherus, Patricia C. Jost,*,§ John R. Silvius, and Lowell E. Hokin

ABSTRACT: Phospholipids at the lipid–protein interface of membrane proteins are in dynamic equilibrium with fluid bilayer. In order to express the number of binding sites (N) and the relative binding constants (K) in terms of measurable quantities, the equilibrium is formulated as an exchange reaction between lipid molecules competing for hydrophobic sites on the protein surface. Experimental data are reported on two integral membrane proteins, cytochrome oxidase and (Na,K)-ATPase, reconstituted into defined phospholipids. Electron spin resonance measurements on reconstituted preparations of beef heart cytochrome oxidase in 1,2-dioleoyl-*sn*-3-phosphatidylcholine containing small quantities of the spin-labeled phospholipid 1-palmitoyl-2-(14-proxylstearoyl)-*sn*-3-phosphatidylcholine (PC*) gave a linear plot of bilayer/bound PC* vs. the lipid/protein ratio as predicted by the theory, with $K \simeq 1$ and $N = 40$ (normalized to heme aa_3). This demonstrates that the spin-label moiety attached to the hydrocarbon chain does not significantly perturb the binding equilibria. In the second experimental system, (Na,K)-ATPase purified from rectal glands of *Squalus acanthias* was reconstituted with defined phosphatidylcholines as the lipid solvent and spin-labeled phospholipids with choline or serine head groups (PC*, PS*) as the solute. The (Na,K)-ATPase has a larger number of lipid binding or contact sites ($N = 60$–65 per $\alpha_2\beta_2$ dimer) and exhibits a detectably larger average binding constant for the negatively charged phosphatidylserine than for the corresponding phosphatidylcholine. These results show that a multiple equilibria, noninteracting site binding treatment can account for the behavior of lipids exchanging between the protein surface and the lipid bilayer. Selective sites among a background of nonselective sites are experimentally detectable as a change in the measured relative binding constant.

Membrane proteins penetrating the lipid bilayer experience two solvent systems: the binding of water and water-soluble ligands by the hydrophilic regions protruding from the bilayer and the binding or contact of lipids by the hydrophobic regions. The binding of water-soluble ligands to the hydrophilic regions of the membrane protein is formally the same as binding to water-soluble proteins, for which there are well-established treatments (Steinhard & Reynolds, 1969; Klotz & Hunston, 1971).

The problem of determining the equilibrium distribution of the various lipid species between the hydrophobic protein surface and the lipid bilayer has received very little attention in the literature. The influence of lipid composition on the function of membrane proteins is likely to be greatest at the lipid–protein interface, and several effects of lipid composition on membrane protein activities have been reported (Sandermann, 1978).

Until the introduction of appropriate techniques, it was not possible to determine which lipids are in contact with the proteins because the two phases cannot be physically separated as is the case in classical enzymology. With the introduction of electron spin resonance (ESR)[1] spectroscopy of spin-labeled lipids, it has become possible to distinguish the protein-associated lipids from the bilayer lipids without macroscopic separation of the two species (Jost et al., 1973; Jost & Griffith, 1978). Recently, preliminary spin-labeling data have been reported that indicate some selectivity for the polar head group (Birrell et al., 1978; Brotherus et al., 1980; Marsh & Watts, 1982). Differential scanning calorimetry (Boggs et al., 1977), Raman spectroscopy (Taraschi & Mendelsohn, 1980), fluorescence spectroscopy (Kimelman et al., 1979), and nuclear magnetic resonance spectroscopy (Van Zoelen et al., 1978; Seelig & Seelig, 1978; Kang et al., 1979; Utsumi et al., 1980; Paddy et al., 1981; Yeagle & Romans, 1981) also show promise in characterizing lipid distributions.

The present work focuses on the dynamic equilibrium occurring within the membrane. The classical multiple equilibrium binding treatment is rederived in a form useful for extracting equilibrium constants and related thermodynamic parameters from spin-labeling and other related lipid binding data. As in the case of virtually all of the familiar equilibrium binding treatments developed for biochemistry, the basic thermodynamic formalism is not new. The membrane problem differs from that of the usual binding site equilibrium of water-soluble proteins or detergent-solubilized systems because (1) different experimental variables are measured in the membrane continuum and (2) the effective concentration of membrane proteins in the lipid solution is high. The analytical expressions derived for the general case and simplifying approximations, together with computer-generated plots for the most relevant limiting cases, are presented. This treatment is used to analyze experimental spin-labeling data from two

† From the Department of Medical Chemistry, University of Helsinki, Siltavuorengpenger 10, 00170 Helsinki 17, Finland (J.R.B. and M.O.B.), the Institute of Molecular Biology, University of Oregon, Eugene, Oregon 97403 (O.H.G., P.C.J., and J.R.S.), and the Department of Pharmacology, University of Wisconsin, Madison, Wisconsin 53706 (L.E.H.). *Received October 14, 1980; revised manuscript received April 2, 1981.* This work was supported by Grants GM 25698 (O.H.G. and P.C.J.) and HL 16318 (L.E.H.) from the U.S. Public Health Service and by the Finnish Academy (J.R.B.). J.R.S. is a fellow of the Medical Research Council of Canada. A preliminary report of some of this work has been presented (Griffith & Jost, 1979).

‡ It is with great sadness and a deep feeling of both personal and scientific loss that we notify the readers that Dr. Jaakko R. Brotherus died on June 11, 1981, in Helsinki at the age of 36 after a sudden brief illness. For those who did not know him personally, we can only say that he was a gentle, joyful, and delightful person as well as an exceptionally talented scientist.

§ To whom reprint requests should be addressed.

[1] Abbreviations used: ESR, electron spin resonance; PC, phosphatidylcholine; DOPC, 1,2-dioleoyl-*sn*-3-phosphatidylcholine; DEPC, 1,2-dielaidoyl-*sn*-3-phosphatidylcholine; POPC, 1-palmitoyl-2-oleoyl-*sn*-3-phosphatidylcholine; PC*, 1-palmitoyl-2-(14-proxylstearoyl)-*sn*-3-phosphatidylcholine; PS*, 1-palmitoyl-2-(14-proxylstearoyl)-*sn*-3-phosphatidylserine; proxyl, 2,2-disubstituted 5,5-dimethylpyrrolidinyl-*N*-oxy; cytochrome oxidase, cytochrome *c* oxidase (EC 1.9.3.1); (Na,K)-ATPase, ATP phosphohydrolase (EC 3.6.1.3).

0006-2960/81/0420-5261$01.25/0

representative integral membrane proteins reconstituted in defined lipids.

Materials and Methods

Lipid-poor cytochrome oxidase was prepared by the method of Yu et al. (1975) and stored at −196 °C in 1% cholate, 0.25 M sucrose, 50 mM phosphate, and 1 mM EDTA, pH 7.4. The phospholipid spin-labels were prepared by using the procedures of Keana (1979). Reconstitution was accomplished with varying amounts of lipid (DOPC) containing low levels of the spin-label (PC*) solubilized in the same cholate-containing buffer. Subsequent removal of cholate by dialysis or sucrose-gradient centrifugation, using cholate-free buffer, yielded vesicular structures as visualized by electron microscopy of negatively stained aliquots. The samples were concentrated for ESR experiments by centrifugation. The lipid-poor enzyme, containing 11 nmol of heme *a* per mg of protein, was assayed by the method of Kuboyama et al. (1972) and had an activity of ~230 nmol of O_2 s^{-1} mg^{-1} with added DOPC and Emasol 1130, 60 μM cytochrome *c*, 30 mM ascorbate, 0.7 mM EDTA, and 50 mM phosphate, pH 7.4. The final reconstituted samples, when resolubilized and assayed under the same conditions, showed no loss of activity within experimental error.

Lipid-rich (Na,K)-ATPase was purified from rectal glands of *Squalus acanthias* by the method of Dixon & Hokin (1978), and lipid substitution followed the general method of Warren et al. (1974) as modified by Hilden & Hokin (1976), except that the buffer was 0.25 M sucrose, 1 M KCl, 20 mM NaCl, 30 mM imidazole, 1 mM cysteine, 1 mM dithiothreitol, 1 mM ATP, and 1 mM EDTA, pH 7.0, and the sample was not vortexed. Two steps of lipid substitution (first step, 6–8 mg of enzyme, 30 μmol of PC, and 80 μmol of cholate; second step, 30 μmol of PC and 65 μmol of cholate) were followed by adding the desired spin-label (at <2 labels/$\alpha_2\beta_2$ ATPase unit, assuming a molecular weight of 314 000) and varying amounts of unlabeled lipid in cholate at 0 °C with DOPC or at 10 °C with DEPC. The mixture was diluted 2-fold and the cholate reduced to <1 mol/mol of ATPase $\alpha_2\beta_2$ units (determined as [^{3}H]cholate) by gel chromatography on Sephadex G-50. Void volume fractions were centifuged through 15% sucrose, 1 mM Tris, 1 mM EDTA, and 0.5 mM dithiothreitol, pH 7.0, onto a buffered 55% sucrose pad, resuspended in buffered 15% sucrose, and centrifuged again to concentrate the sample for ESR measurements. Quantitative thin-layer chromatography showed ≤1 mol of residual non-PC phospholipid per mol of ATPase $\alpha_2\beta_2$ units. The final preparation had a basal activity of ~4 μmol of phosphate min^{-1} mg^{-1} when assayed as previously described (Brotherus et al., 1979), which was stimulated approximately 2.5-fold by preincubation with a 10-fold excess of asolectin.

The methods of ESR data analysis, integration and spectral analysis, were as described by Jost & Griffith (1978), except that final endpoints in the spectral titrations were selected by comparing bilayer difference spectra with experimental spectra recorded as a function of temperature from vesicles containing the appropriate phospholipid and spin-label at a lipid:spin-label ratio of 150:1.

Theory

A Form of the General Equation for Multiple Independent Binding Sites Appropriate for Membrane Equilibria. Consider a fluid lipid bilayer consisting of two molecular species, solvent L and solute L*, and a membrane protein P that contains m classes of lipid binding sites B_i (i = 1, ..., m) on its hydrophobic surface, each class being able to bind n_i lipid molecules. The exchange equilibrium of the two types of lipid between the bialyer and a single site on the protein is described as

$$B_iL + L^* \rightleftharpoons B_iL^* + L$$

The chemical potential of the solute lipid in the bilayer is of the form $\mu_{L^*,f} = \mu^\circ_{L^*,f} + RT \ln (\gamma_{L^*,f}X_{L^*,f})$ where $X_{L^*,f}$ is the mole fraction of the free solute lipid in the bilayer, $X_{L^*,f} = L^*_f/(L_f + L^*_f)$, $\gamma_{L^*,f}$ is the activity coefficient of the free solute lipid, and L^*_f and L_f are the moles of free solute lipid and free solvent lipid in the bilayer, respectively. Similarly, the chemical potential of solute lipid bound to the ith class of protein sites is $\mu_{L^*,b_i} = \mu^\circ_{L^*,b_i} + RT \ln (\gamma_{L^*,b_i}X_{L^*,b_i})$ where $X_{L^*,b_i} = L^*_{b_i}/(L_{b_i} + L^*_{b_i})$, γ_{L^*,b_i} is the activity coefficient of the bound solute lipid, and $L^*_{b_i}$ and L_{b_i} are the moles of solute lipid and solvent lipid, respectively, bound to the protein sites B_i. There are two analogous expressions for the chemical potential of the free and bound solvent lipid. Each standard chemical potential, μ°, contains contributions from the internal free energies of L or L* and contributions from the interaction of the lipid with its neighbors in the standard state.[2] The aqueous concentrations do not enter into these expressions explicitly because the problem is formulated as an exchange occurring within the hydrophobic bilayer (the monomeric solubility of L and L* in water is very small). At equilibrium, $\Delta\mu_i = (\mu_{L^*,b_i} + \mu_{L,f}) - (\mu_{L,b_i} + \mu_{L^*,f}) = 0$, and the standard free-energy change ΔG°_i (or $\Delta\mu^\circ_i$) is $\Delta G^\circ_i = -RT \ln K_i$ where the relative binding constant K_i is

$$K_i = \left(\frac{X_{L^*,b_i}X_{L,f}}{X_{L,b_i}X_{L^*,f}}\right)\left(\frac{\gamma_{L^*,b_i}\gamma_{L,f}}{\gamma_{L,b_i}\gamma_{L^*,f}}\right)$$

Since the exchange reaction is one to one, the denominators in the mole fractions cancel, and all quantities can be expressed as moles, so that

$$K_i = \left(\frac{L^*_{b_i}L_f}{L_{b_i}L^*_f}\right)R_\gamma \qquad (1)$$

where R_γ represents the ratio of the activity coefficients in the above equation.

The following assumptions are made in order to derive useful simplified equations: (1) the individual binding sties are noninteracting; (2) all binding constants of a given class K_i are equivalent; (3) the ratio of the activity coefficients in eq 1 is unity; (4) the problem can be formulated as an exchange equilibrium in which there are no unoccupied lipid binding sites (all sites are occupied by either L or L*); (5) the membrane sample is a homogeneous population of lipid and protein; (6) all positions in the fluid bilayer can be treated as equivalent; (7) the fluid bilayer is above the gel to liquid-crystalline phase transition; (8) there is complete mixing of L and L* in the fluid bilayer phase; (9) there exists a method of detecting the difference between the solute lipid bound to the protein and the solute lipid (L^*_f) surrounded by other lipids in the fluid bilayer. Detection of bound and free solvent lipid is not assumed. Assumptions 1–3 are the usual starting points for multiple equilibrium binding treatments in aqueous soltuion.

The remaining relevant properties of the system are described by the conservation equations:

binding sites

$$L_{b_i} + L^*_{b_i} = n_iP \qquad (2)$$

[2] The standard state of the solvent lipid in the bilayer is the pure solvent lipid bilayer. The standard state for the solute lipid in the bilayer is chosen so that the activity becomes equal to the mole fraction ($\gamma_{L^*,f} \rightarrow 1$) as the mole fraction of solute lipid in the bilayer approaches zero.

solute

$$L^*_f + \sum_{i=1}^{m} L^*_{b_i} = L^*_t \quad (3)$$

solvent

$$L_f + \sum_{i=1}^{m} L_{b_i} = L_t \quad (4)$$

where L_t = total solvent lipid concentration, L^*_t = total solute lipid concentration, P = total protein concentration, and n_i = number of binding sites of class i per protein.

Equations 1–4 form a set of $2m + 2$ independent (but nonlinear) equations from which the $2m + 2$ variables ($L^*_{b_i}$, L_{b_i}, L^*_f, and L_f) can be solved in terms of the constants of the system (L^*_t, L_t, P, n_i, K_i, and N) where N is the total number of binding sites per protein. The most important variable is the amount of free solute lipid (L^*_f). Therefore, the following strategy is adopted to eliminate the other variables first.

Solving eq 1 for $L^*_{b_i}$ and eliminating L_{b_i} by using eq 2 give

$$L^*_{b_i} = \frac{n_i K_i P (L^*_f / L_f)}{1 + K_i (L^*_f / L_f)} \quad (5)$$

Substituting eq 5 into eq 3 and rearranging terms give

$$\frac{L^*_t - L^*_f}{P} = \bar{\nu} = \sum_{i=1}^{m} \frac{n_i K_i (L^*_f / L_f)}{1 + K_i (L^*_f / L_f)} \quad (6)$$

where $\bar{\nu}$ (also called r) is the bound solute/protein ratio. This form of the general binding equation is useful in cases where L_f as well as L^*_f can be measured directly (in principle, in some differential scanning calorimetric and spectroscopic experiments). However, in the conventional spin-labeling experiment, L^*_f, but not L_f, is measured directly. In order to eliminate L_f, we note that the total amount of free bilayer in the system is $L_t + L^*_t - NP$, where NP (i.e., $N \times P$) is the total number of binding sites in the system. Therefore, the concentration of free solvent in the bilayer (L_f) is[3]

$$L_f = L_t + L^*_t - NP - L^*_f \quad (7)$$

Substituting eq 7 into eq 6 and simplifying yield

$$\frac{L^*_t - L^*_f}{P} = \sum_{i=1}^{m} \frac{n_i K_i}{[(L_t + L^*_t - NP - L^*_f)/L^*_f] + K_i} \quad (8)$$

Finally, defining x to be the total solute lipid/protein ratio, $x = L_t/P$; x^* to be the total solute lipid/protein ratio, $x^* = L^*_t/P$; and y to be the bilayer/bound ratio for the solute lipid, $y = L^*_f/(L^*_t - L^*_f)$, and rearranging terms give

$$\sum_{i=1}^{m} \frac{n_i K_i y}{(1 + K_i y)(1 + y)^{-1} x^* + x - N} = 1 \quad (9)$$

which can also be rearranged into a polynomial of degree $m + 1$. Equation 9 is symmetrical in that the roles of L_f and L^*_f can be interchanged, and there are no theoretical restrictions on the relative amounts of solute, solvent, and protein, other than that all sites are occupied by lipid. The experimentally observed variable chosen here is the ratio of free (bilayer) to bound solute because this quantity is most readily obtained in the ESR experiment. Other possible choices besides $\bar{\nu}$ and y include the ratio of free solute to total solute, L^*_f/L^*_t, and the ratio of bound solute to total solute, $(L^*_t - L^*_f)/L^*_t$. Similarly, the concentration variables (x, x^*) can be replaced by others, for instance, the total lipid to protein ratio ($x + x^*$) or the mole ratios of protein to lipid (i.e., $1/x$ and $1/x^*$). These alternative choices lead to slightly different formulations of the general eq 9.

Comparison with Equations for Ligand Binding to Water-Soluble Proteins. Equation 6 is readily reduced to the familiar form of the binding equation by replacing the mole ratio L^*_f/L_f by the concentration of free solute $[L^*_f]$ in moles per liter of solution. This approximation is valid for typical solution binding studies where $L_f \approx L_t$, because of the large excess of solvent. In this limit, eq 6 becomes

$$\bar{\nu}_t = \frac{n_1 K_1 [L^*_f]}{1 + K_1 [L^*_f]} + \frac{n_2 K_2 [L^*_f]}{1 + K_2 [L^*_f]} + \ldots + \frac{n_m K_m [L^*_f]}{1 + K_m [L^*_f]} \quad (10)$$

where K now contains the concentration of water ($\leq$55 M) and solvent lipid. For the case of one class of binding sites, eq 10 becomes the familiar relation $1/\bar{\nu} = 1/n + 1/(nK[L^*_f])$ (Steinhard & Reynolds, 1969; Klotz & Hunston, 1971). However, this equation is not appropriate since a significant fraction of the total lipid is at the lipid–protein interface in most membranes (Jost & Griffith, 1980).

Limiting Approximations at Low Solute Levels. In most labeling experiments, the solute concentration (x^*) is kept low. Under these conditions, a useful limiting case is to assume that the terms containing x^* in eq 9 are so small that they can be neglected, i.e., $(1 + K_i y)(1 + y)^{-1} x^* \ll x - N$. It follows that $\sum_{i=1}^{m} n_i K_i y/(x - N) = N K_{av} y/(x - N)$ where

$$K_{av} = \sum_{i=1}^{m} n_i K_i / N \quad (11)$$

K_{av} is the average of all individual binding constants. This equation can be rewritten as

approximation I

$$y = \frac{x}{N K_{av}} - \frac{1}{K_{av}} \quad (12)$$

so that a graph of y vs. x is a straight line with a slope of $1/(NK_{av})$, a y intercept of $-1/K_{av}$, and an x intercept of N. This behavior is identical with that of the case of one class of binding sites (see below).

At somewhat higher values of x^*, a better approximation is

approximation II

$$y = \frac{x + x^*}{N K_{av}} - \frac{1}{K_{av}} \quad (13)$$

This follows from eq 9 by setting $(1 + K_i y)(1 + y)^{-1} x^* \approx x^*$. Equation 13 is a linear relationship between x and y and has the same x-axis intercept ($N - x^*$) as that of the general eq 9.

One Class of Binding Sites. When all protein binding sites are identical, only one term of eq 9 remains, and this can be simplified to

$$\frac{x^*}{1 + y} + \frac{x}{1 + Ky} = N \quad (14)$$

The terms of this equation have simple physical interpretations: $x^*/(1 + y)$ is the average occupancy of the protein by the solute ($\bar{\nu}$), and $x/(1 + Ky)$ is the average occupancy by the solvent lipid ($N - \bar{\nu}$).

Equation 14 is equivalent to a second-degree polynomial equation in y. At low solute lipid concentrations, it reduces to the same two linear approximations I and II as for the

[3] Equation 7 cal also be derived by combining eq 2–4.

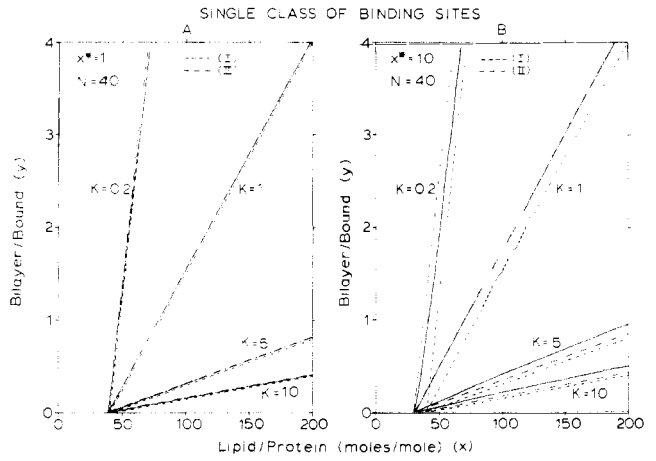

FIGURE 1: Calculated binding curves for one class of binding sites as a function of the solvent lipid to protein ratio (x). Solid lines are plots of the exact eq 9, and I and II refer to the approximate solutions eq 12 and 13, respectively. For this particular example, the total number of binding sites (N) equals 40, and the solute to protein ratio (x^*) is 1 (A) and 10 (B). The binding constant (K) is varied between 0.2 and 10.

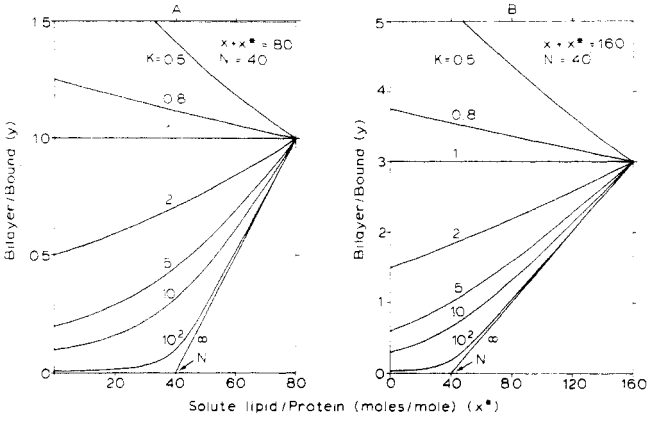

FIGURE 2: Calculated binding curves for one class of binding sites as a function of the solute lipid to protein ratio (x^*). This is the same case as in Figure 1 but with the total lipid ($x + x^*$) held constant at 80 molecules/protein (A) and 160 molecules/protein (B).

general case, except that K_{av} becomes K, the binding constant of the single class.

Other linear approximations to eq 14 can be derived, including, for example, $y = x/(NK) + x^*/N - 1/K$ and $y = (x + x^* - N)/[(N - x^*)K + x^*]$. By analogy with the Scatchard and double -reciprocal equations for classical binding equilibria, there are other ways of graphing the data to yield useful linear plots. For example, rearranging eq 12 with K replacing K_{av} and plotting y/x vs. $1/x$ give a line with a slope of $-1/K$, an intercept on the abscissa of $1/N$, and an intercept on the ordinate of $1/(NK)$. This plot resembles the familiar Scatchard plot in that it has a negative slope. For more than one class of binding sites, this resemblance disappears.

The effect of the binding constant on the calculated ratio of free to bound solute (y) is shown in Figure 1 as a function of the lipid to protein ratio (x). The exact solution and two linear approximations are plotted in this figure. The horizontal axis corresponds to the case $K = \infty$ and the vertical axis to $K = 0$.

Plots in Figure 2 show the dependence of the binding ratio (y) on the solute lipid to protein ratio (x^*) for the same system as in Figure 1. All curves of Figure 2A or 2B approach the same point as the lipid mixture approaches 100% solute, since at this point the solute molecules are competing only with other solute molecules. The lower left quadrant of each set of curves

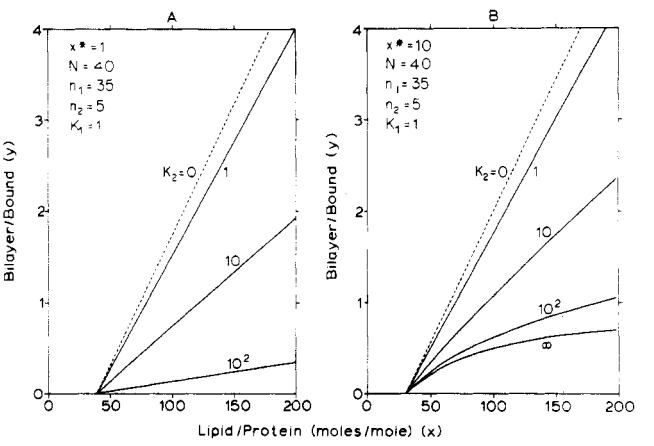

FIGURE 3: Calculated binding curves for two classes of binding sites as a function of the solvent lipid to protein ratio (x) with five selective sites (n_2) and the remaining 35 sites (n_1) nonselective ($K_1 = 1$). The total number of sites (N) is 40, and the solute to protein ratio (x^*) is 1 (A) and 10 (B). The excluded site case ($K_2 = 0$) is shown by dashed lines.

shows the correct limiting behavior; i.e., for very high binding constants, the amount of free solute lipid remains very low until all sites are saturated, after which all added solute remains in the bilayer.

Two Classes of Binding Sites. For this biologically interesting case, eq 9 becomes

$$\frac{n_1K_1y}{(1 + K_1y)(1 + y)^{-1}x^* + x - N} + \frac{n_2K_2y}{(1 + K_2y)(1 + y)^{-1}x^* + x - N} = 1 \quad (15)$$

Equation 15 is useful in analyzing data when there is selectivity in lipid–protein interactions, for example, if most of the sites represent transient contact sites between the lipid and protein, and only a few sites exhibit specificity for the geometry or charge of the lipid polar head group.

In Figure 3, binding isotherms are plotted for one selective class of sites with varying binding constants (K_2). For the nonselective sites, the binding constant (K_1) is equal to 1. The curves are calculated by using eq 15. At low solute level (Figure 3A), the binding curves are essentially linear and resemble the curves of Figure 1A. The x intercept is still N, because at low lipid levels all solute molecules will bind to (or contact) the protein. The slopes for the one- and two-class cases are the same for $K = 1$, but in the two-class case, the slope decreases more slowly with increasing binding constant, because the slope is inversely related to the average of all binding site affinities (see eq 11). If the solute concentration level is increased well above the number of the selective sites, the curves become markedly nonlinear (Figure 3B). For an equivalent number of solute molecules (x^*), the curvature is much greater than that for the single class case. Thus, these two cases are distinguishable at higher solute levels.

In Figure 4, the binding curves for the two-class case are plotted as a function of the solute to protein ratio (x^*) for two different numbers of selective binding sites. These curves differ from those in Figure 2 in that they become convex at values of $x^* > n_2$ (for $K_2 > 1$). Another difference is that, for high binding constants, the region of high curvature is in the neighborhood of n_2, well below the total number of binding sites (N).

Excluded Sites and Nonexchangeable Lipid. Excluded sites are sites that bind the solvent but have a zero binding affinity for the solute ($K_2 = 0$). For eq 15, if $K_2 = 0$, the first term

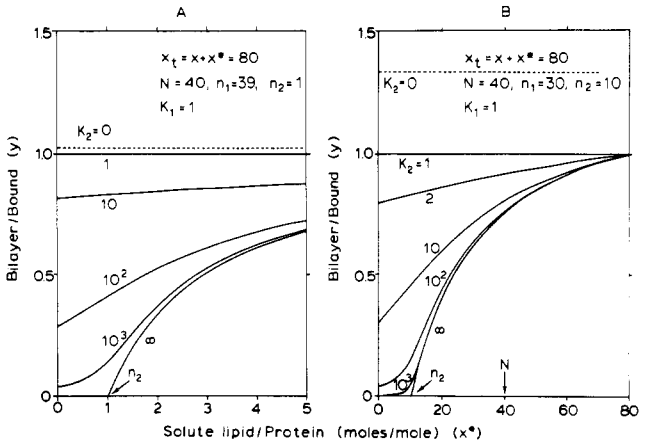

FIGURE 4: Calculated binding curves for the two-class model as a function of the solute to protein ratio (x^*). The number of specific binding sites is 1 (A) and 10 (B), and the total number of sites in both plots is 40. The total lipid ($x + x^*$) is held constant at 80 molecules/protein. As in Figure 3, $K_1 = 1$ for the nonspecific sites. The excluded site case ($K_2 = 0$) is shown by dashed lines.

vanishes, and at the limit of low solute levels, the equation becomes $y = x/[(N - n_2)K_1] - N/[(N - n_2)K_1]$, where n_2 is the number of excluded sites. The x intercept is still N, the same as that for cases where all sites are accessible (the exact intercept is still $N - x^*$). The slope of the curve of y vs. x is larger for the excluded site case. [Another way of showing this is from eq 11: $NK_{av} = (N - n_2)K_1 + n_2(0) = (N - n_2)K_1 < NK_1$.] The examples of $K_2 = 0$ curves are shown as dashed lines in Figures 3 and 4.

Nonexchangeable lipid, by definition, does not exchange with either the solvent or the solute lipid. For example, nonexchangeable lipid will occur experimentally if the membrane protein has some high-affinity binding sites occupied by a lipid species that differs from both the added solvent and solute lipids. If the nonexchangeable lipid is not extracted and/or measured by chemical analysis, and hence does not appear in x, then the x intercept remains the value of the number of sites involved in equilibrium binding. However, if the nonexchangeable lipid is measured in the total lipid, then this case is technically the same as the excluded site case both in the x intercept and in the slope. The extrapolated value of N will include both the nonexchangeable sites (n_2) and the equilibrium binding sites. The excluded site case may occur in a reconstituted system, depending on the choice of the solute and solvent lipids.

Results

Cytochrome Oxidase. An experimental binding curve for this mitochondrial integral membrane protein reconstituted in phosphatidylcholine vesicles is shown in Figure 5. The experimental design involved reconstituting beef heart cytochrome oxidase with DOPC containing a low level of spin-labeled PC (PC*). The ESR spectra exhibited two components, one characteristic of the fluid bilayer and the other motion-restricted. The motion-restricted spectral component is present only when the protein is present, and there is considerable evidence from previous studies using similar phospholipid and fatty acid spin-labels that this spectal component represents lipid in direct contact with the protein (Jost et al., 1973; Jost & Griffith, 1978; Birrell et al., 1978; Brotherus et al., 1980; Marsh & Watts, 1982). The narrower spectral component is characteristic of lipid bilayers, and there is essentially no label in the aqueous phase in which the vesicles are suspended. We take the ratio of the integrated intensities of the bilayer component to the motion-restricted component

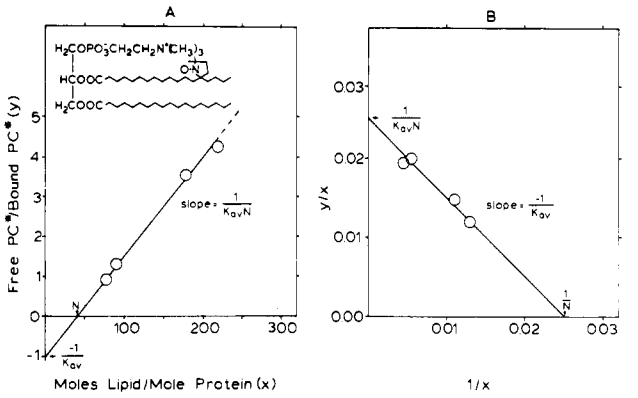

FIGURE 5: Experimental binding curve at 25 °C for beef heart cytochrome oxidase reconstituted in phosphatidylcholine (solvent lipid) containing low levels of a phosphatidylcholine spin-label (solute lipid). (A) Plot of y vs. x with $K_{av} = 1$ and $N = 40$ (eq 12); (B) the same data plotted as y/x vs. $1/x$.

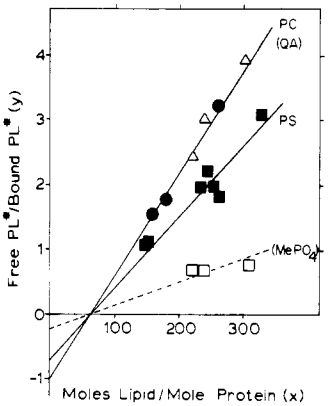

FIGURE 6: Experimental solute lipid binding curves at 25 °C for (Na,K)-ATPase reconstituted with pure PC (DOPC or DEPC) as the solvent and low levels of PC* (closed circles) or PS* (closed squares) as the solute lipid at <2 labels per $\alpha_2\beta_2$ functional unit (see Materials and Methods). For comparison, data reported by Griffith et al. (1982) for the binding of charged long-chain amphiphiles to the shark enzyme in a POPC background are plotted as well: positively charged quaternary amine lipid label (QA, open triangles) and negatively charged methyl phosphate lipid label ($MePO_4$, open squares). The dashed line is calculated for $K_{av} = 4.5$ to fit N for our data. Note the closely similar behavior of the cationic (QA) and neutral (PC) spin-labels, which differs from the behavior of the negatively charged lipid labels (PS and $MePO_4$).

as the free to bound ratio, y. Figure 5A shows the resulting plot of y vs. x, the molar ratio of phospholipid to protein. The curve is linear, and it has an x-axis intercept of $N = 40$ (given 5.5 mol of heme aa_3 per mg of protein). The slope of the curve coincides, within experimental error, with the $K = 1$ line[4] of eq 12. Figure 5B shows a plot of y/x vs. $1/x$ using the same data, and again the points fall on the line corresponding to $K = 1$. These data were collected at 25 °C, well above the transition temperature of the bulk lipid.

(Na,K)-ATPase. Experimental binding curves for this transmembranous protein reconstituted in vesicles are shown in Figure 6. The vesicles were doped with low levels of lipids with different polar head groups, each solute lipid labeled with the nitroxide moiety to make it detectable by ESR. The solid symbols compare the behavior of two solutes, the neutral

[4] A small correction may be needed for any nonexchangeable diphosphatidylglycerol (DPG) present in this system. There are approximately two molecules of tightly bound DPG that do not exchange for DOPC during the reconstitution, equivalent to four PC sites. Thus, $NK_{av} = (40)(1) = n_1K_1 + n_2K_2 = (36)K_1 + (0)(4)$. Thus, $K_1 = 40/36 = 1.1$. This value cannot be distinguished from 1.0 within experimental error.

phosphatidylcholine (PC) and the negatively charged phosphatidylserine (PS) both in phosphatidylcholine as the solvent lipid. The solid lines correspond to $K_{av} = 1$, $N = 64$ for PC and $K_{av} = 1.5$, $N = 64$ for PS. Since moles of lipid per mole of protein is calculated for a protein molecular weight of 314 000, the number of binding sites (N) refers to the $\alpha_2\beta_2$ dimer. The remaining data are for two single-chain lipids with different polar head groups, replotted from Griffith et al. (1982). In these single-chain amphiphilic labels, a 14-proxyloctadecyl chain (resembling the β chain of the lipid shown at the top of Figure 5A) is attached to either a positively charged quaternary amine (Figure 6, open triangles) or a negatively charged methyl phosphate moiety (Figure 6, open squares). The dashed line associated with the methyl phosphate data points corresponds to $N = 64$ and $K_{av} = 4.5$, while the quaternary amine data approximately fall on the $N = 64$ and $K_{av} = 1$ line.

Discussion

Beginning with the plausible assumption that the multiple lipid–protein binding in membranes can be treated as an exchange reaction with the phospholipid bilayer, we derived two types of useful formulas. One describes the general case (eq 9) for the lipid–protein associations over a wide range of solute lipid concentrations. The other type (eq 12 and 13) is linearized equations that are easier to use and apply when the solute lipid concentration is low. This is the most frequently encountered case in labeling experiments. The experimental quantities needed are the lipid/protein ratio of the membrane system determined chemically, and a measure of the amount of solute lipid associated with the protein. This can be estimated, for example, by ESR using spin-labeled solute lipids.

The predicted behavior of the bilayer/bound solute ratio, y, is sensitive to the value of the relative binding constant K and gives the number of binding sites N directly, as illustrated in Figure 1 for the single class of sites case.[5] Figure 1 also shows the accuracy of the linear approximations I and II compared to the exact solution (solid line). At low solute levels, for example, one solute molecule per protein ($x^* = 1$ in Figure 1A), all three curves are very nearly superimposable for all values of K, and the intercept is essentially N. Even when the solute level is increased 10-fold, both approximations are still reasonably good (Figure 1B). Both have the same slopes, and approximation II gives the same x-axis intercept as that of the exact solution ($N - x^*$). Approximation I is easier to apply because it does not require the exact knowledge of the solute concentration other than that it is low with respect to the protein. The effect of progressively higher solute concentrations for fixed lipid/protein ratios is shown in Figure 2.

When all sites are not equivalent, which is the case one would predict for many membrane proteins, the two classes of sites treatment is the simplest starting point for describing the system. It is useful and important that the same types of plots are obtained regardless of the number of classes of sites, when the labeling level (solute) is low. Thus, without knowledge of the number of classes of sites or the exact solute to protein ratio (x^*), a plot of y vs. x will be essentially linear and gives the weighted average of the relative binding constants, K_{av}, and the total number of binding sites, N. This follows from the general eq 9, neglecting terms in x^*. Approximation I is again the most useful form, even when an unknown number of classes of binding sites is involved. Plots of this type are shown in Figure 3. To proceed further and determine the number of sites and binding constants for each class of sites, the experimental design must be changed to vary the moles of solute lipid per mole of protein. This is equivalent to a saturation of sites experiment (Langmuir isotherm). Theoretical plots for one class of sites and two classes of sites are shown in Figures 2 and 4. In the absence of these kinds of data, which are experimentally more troublesome to obtain, some additional information about the system can be obtained at low values of x^* if a series of solutes that differ in the polar head groups are used.

The experimental applications reported here were designed to test three things: (1) whether linear plots can be obtained as predicted by the theory; (2) whether attachment of the spin-label moiety near the end of one acyl chain on the solute phospholipid affects the relative binding constant; and (3) whether or not there is any polar head-group selectivity in the lipid–protein association.

For both experimental systems, cytochrome oxidase (Figure 5) and (Na,K)-ATPase (Figure 6), plots were obtained that are linear within experimental error over the range of lipid/protein ratios, as predicted by the theory. These linear plots also provide evidence that there is no large-scale protein aggregation that traps variable amounts of labeled lipid as the protein concentration is decreased. Such aggregation would almost certainly produce significant nonlinearities.

The attachment of labels can, in principle, alter the lipid–protein association. A solute lipid is used that has the same polar head group as that of the solvent to test whether this effect is significant with the labels used here. The result should be a measured relative binding constant $K_{av} \simeq 1$, regardless of the number and types of sites present. The experimental result is that, when both the solute and solvent lipids are phosphatidylcholines, the value of the binding constant for the labeled lipid relative to that for the unlabeled lipid is approximately equal to 1 (see Figure 5 and the top curve of Figure 6). This result is consistent with earlier data on cytochrome oxidase (Griffith & Jost, 1979; Jost et al., 1973; Knowles et al., 1979). We conclude that the presence of the spin-label moiety does not significantly enhance or inhibit the phosphatidylcholine association. Therefore, the phosphatidylcholine spin-label is faithfully reflecting the behavior of the unlabeled phosphatidylcholine. This result is significant both for experiments to evaluate the number of sites (N) and potential selectivity (K_{av}) using low levels of solute and for designing experiments to determine the number of selective sites by saturating the sites. In the latter case, the troublesome consequences of high concentrations of pure labels, such as exchange and dipolar interactions between spins or quenching of fluorescence labels, can be circumvented by successively diluting the labeled solute with unlabeled solute lipid.

The total number of lipid binding sites obtained from these data is consistent with the idea that there is a substantial hydrophobic surface area of these proteins that interacts with lipids in the bilayer. The number obtained from the experimental data for the beef heart cytochrome oxidase monomer is consistent with the earlier method that assumed $K = 1$ (Jost et al., 1973) and approximates the slightly higher number estimated for the yeast cytochrome oxidase (Knowles et al., 1979). The total number of binding sites for the shark ATPase is consistent with that obtained in an earlier study of the electric eel (Na,K)-ATPase studied as a function of salt suppression of specific binding rather than as a function of the lipid/protein ratio. While the number of binding sites for

[5] It should be noted that the measurement of a relative binding constant does not necessarily imply specific sites with high-affinity binding. Transient contact sites between lipid and protein are included as binding sites, providing they are detected by the experimental technique.

the functional dimer was earlier estimated as being on the order of 61 (Brotherus et al., 1980), the equilibrium binding method presented here is more generally useful and reliable in determining the number of binding sites, and in addition provides the average relative binding constants.

In the case of (Na,K)-ATPase where different solute lipids have been used in the phosphatidylcholine solvent, the data show a change in the average relative binding constant, K_{av}. The value of K_{av} is detectably higher for phosphatidylserine ($K_{av} \sim 1.5$) than for phosphatidylcholine.

Other data for a single tail lipid label carrying a positive charge (quaternary amine) also fall on the $K_{av} \sim 1$ line, while the corresponding negatively charged lipid (methyl phosphate) shows the greatest selective binding, with $K_{av} \sim 4.5$ (Figure 6). There is clearly some charge preference in the (Na,K)-ATPase system.

An increase in K_{av} can be the result either of a small number of sites with a higher selective binding constant or of a large number of sites with a much smaller affinity for the negatively charged lipids. The maximum value of the selective binding consistent with the measured value of $K_{av} \sim 4.5$ for the methyl phosphate label occurs when there is only one selective binding site per ATPase $\alpha_2\beta_2$ functional unit. Since $NK_{av} = n_1K_1 + n_2K_2$, then $(64)(4.5) = (63)(1) + (1)(K_2)$, giving $K_2 = 225$, corresponding to a ΔG of about -3 kcal/mol. Similarly, for PS, the maximum value is $K_2 = 33$ ($\Delta G \sim -2$ kcal/mol). Thus, the value of K_{av} need not be very large to indicate substantial binding constants when the number of selective binding sites is small. At the other extreme, if all of the binding sites are the same and have a limited uniform preference for the negatively charged lipids, then $K_{av} = K$.

The similarity in behavior between the neutral (PC) and the positively charged quaternary amine (QA) with the (Na,K)-ATPase suggests that only a few sites can be selective for negatively charged lipids. Otherwise, the positively charged label would show a diminished interaction with the protein, which would shift the slope of the binding curve to the left of the $K = 1$ line. This is not observed.

Finally, we wish to point out that modest values of lipid binding constants in membranes have the same effect as much larger values of ligand binding constants in aqueous solution because of the concentrated nature of the membrane system. For example, to achieve 90% occupancy of a specific lipid binding site on a protein in a bilayer containing 10 mol % of the specific lipid requires a binding constant (K_2) of 10^2. For comparison, 90% occupancy of a ligand binding site on a water-soluble protein in a dilute solution with an aqueous ligand concentration of 10^{-5} M requires a binding constant on the order of 5×10^7 in comparable mole fraction units.

Acknowledgments

We gratefully acknowledge the contributions of Debra A. McMillen to the experimental work and thank Dr. Tsoo E. King for supplying us with purified cytochrome oxidase and Dr. Johan J. Lindberg for making available facilities for calculations and plotting. We also thank Dr. John F. W. Keana for useful discussions.

References

Birrell, G. B., Sistrom, W. R., & Griffith, O. H. (1978) *Biochemistry 17*, 3768–3773.

Boggs, J. M., Wood, D. D., Moscarello, M. A., & Papahadjopoulos, D. (1977) *Biochemistry 16*, 2325–2329.

Brotherus, J. R., Jost, P. C., Griffith, O. H., & Hokin, L. E. (1979) *Biochemistry 18*, 5043–5050.

Brotherus, J. R., Jost, P. C., Griffith, O. H., Keana, J. F. W., & Hokin, L. E. (1980) *Proc. Natl. Acad. Sci. U.S.A. 77*, 272–276.

Dixon, J. F., & Hokin, L. E. (1978) *Anal. Biochem. 86*, 378–385.

Griffith, O. H., & Jost, P. C. (1979) in *Cytochrome Oxidase* (King, T. E., Orii, Y., Chance, B., & Okunuki, K., Eds.) pp 207–218, Elsevier/North-Holland Biomedical Press, Amsterdam, The Netherlands.

Griffith, O. H., Brotherus, J. R., & Jost, P. C. (1982) in *Lipid–Protein Interactions* (Jost, P. C., & Griffith, O. H., Eds.) Wiley-Interscience, New York (in press).

Hilden, S., & Hokin, L. (1976) *Biochem. Biophys. Res. Commun. 69*, 521–527.

Jost, P. C., & Griffith, O. H. (1978) *Methods Enzymol. 49*, 369–418.

Jost, P. C., & Griffith, O. H. (1980) *Ann. N.Y. Acad. Sci. 348*, 391–407.

Jost, P. C., Griffith, O. H., Capaldi, R. A., & Vanderkooi, G. (1973) *Proc. Natl. Acad. Sci. U.S.A. 70*, 480–484.

Kang, S. Y., Gutowsky, H. S., Hsung, J. C., Jacobs, R., King, T. E., Rice, D., & Oldfield, E. (1979) *Biochemistry 18*, 3257–3267.

Keana, J. F. W. (1979) in *Spin Labeling* (Berliner, L. J., Ed.) Vol. 2, Academic Press, New York.

Kimelman, D., Tecoma, E. S., Wolber, P. K., Hudson, B. S., Wickner, W. T., & Simoni, R. D. (1979) *Biochemistry 18*, 5874–5880.

Klotz, I. M., & Hunston, D. L. (1971) *Biochemistry 10*, 3065–3069.

Knowles, P. F., Watts, A., & Marsh, D. (1979) *Biochemistry 18*, 4480–4887.

Kuboyama, M., Fong, F. C., & King, T. E. (1972) *J. Biol. Chem. 247*, 6375–6383.

Marsh, D., & Watts, A. (1982) in *Lipid–Protein Interactions* (Jost, P. C., & Griffith, O. H., Eds.) Wiley-Interscience, New York (in press).

Paddy, M. R., Dahlquist, F. W., Davis, J. H., & Bloom, M. (1981) *Biochemistry 20*, 3152–3162.

Sandermann, H. (1978) *Biochim. Biophys. Acta 515*, 209–237.

Seelig, A., & Seelig, J. (1978) *Hoppe-Seyler's Z. Physiol. Chem. 359*, 1747–1756.

Steinhard, J., & Reynolds, J. A. (1969) *Multiple Equilibria in Proteins*, Academic Press, New York and London.

Taraschi, T., & Mendelsohn, R. (1980) *Proc. Natl. Acad. Sci. U.S.A. 77*, 2362–2366.

Utsumi, H., Tunggal, B. D., & Stoffel, W. (1980) *Biochemistry 19*, 2385–2390.

Van Zoelen, E. J. J., van Dijck, P. W. M., de Kruijff, B., Verkleij, A. J., & van Deenen, L. L. M. (1978) *Biochim. Biophys. Acta 514*, 9–24.

Warren, G. B., Toon, P. A., Birdsall, N. J. M., Lee, A. G., & Metcalfe, J. C. (1974) *Biochemistry 13*, 5501–5507.

Yeagle, P. L., & Romans, A. Y. (1981) *Biophys. J. 33*, 243–252.

Yu, C., Yu, L., & King, T. E. (1975) *J. Biol. Chem. 250*, 1383–1392.